6th European Conference on Computational Mechanics (ECCM 6)
7th European Conference on Computational Fluid Dynamics (ECFD 7)
11 – 15 June 2018, Glasgow, UK

DYNAMIC ANALYSIS OF A ROTATING SPACE TUBULAR EXTENDABLE BOOM WITH TIP LOAD USING ONE-DIMENSIONAL UNIFIED FORMULATION

YI HU[1], YONG ZHAO[2], LANMIN LI[3], AND ZHOUHUI TUO[4]

[1] National University of Defense Technology
No. 109, Deya Road, Kaifu District, Changsha, China
huyi1185@163.com

[2] National University of Defense Technology
No. 109, Deya Road, Kaifu District, Changsha, China
zhaoyong@nudt.edu.cn

[3] Shandong Institute of Space Electronic Technology
No. 513, Hangtian Road, Hi-tech Industrial Development Zone, Yantai, China
lilm198141@163.com

[4] Chinese Academy of Military Science
No. 2, Fengti South Road, Fengtai District, Beijing, China
13974874321@163.com

Key words: Dynamic Analysis, Rotating structures, Tubular extendable booms, Tip Load, One-dimensional Unified Formulation.

Abstract. Tubular extendable booms, featured by small stowed volume, light weight and large magnification ratios, have greatly promoted the development of spacecraft deployment missions. This paper studies the dynamic characteristics of a rotating tubular extendable boom made by tape spring. The boom deploys a tip load, the MEMS sensor, away from the spacecraft to detect the space environment such as temperature and magnetic field. The dynamic characteristics of the rotating boom are studied by a one-dimensional unified formulation, enhancing the capabilities of beam elements to detect shell-like solutions for the boom. Results show that the natural frequencies of the boom generally increase with the rotating angular velocity. However, they diminish rapidly at the critical velocity, where the first order natural frequency is close to zero and the structure suffers from resonance and large deformation. In addition, the mass effect of the tip load has a serious negative impact on the natural frequencies of the boom, especially the low-order ones. A heavier tip load tends to result in lower natural frequencies and critical velocity. While larger base radius can improve the dynamic characteristics of the rotating boom. The results obtained from this paper can provide reference for the design and control of tubular extendable booms.

1 INTRODUCTION

Space tubular extendable booms is a particular kind of one-dimensional deployable structures featured by small stowed volume, light weight and large magnification ratios.

These booms are widely used as simple and reliable preference for deploying light payloads such as the MEMS sensor to detect the space environment. The mass effect of tip load may seriously influence the dynamic characteristics of the boom and even cause structural resonance. To reduce the probability of structural damage, the dynamic characteristic of the boom with tip load needs to be carefully analyzed by an accurate and efficient method. In this paper, the one-dimensional unified formulation is used to enhance the capabilities of beam elements to detect shell-like dynamic solutions for the rotating boom.

The dynamic analysis of flexible hub-beam system with tip mass is studied by various researchers. Yang[1] presents a finite element model with a second order approximation for the displacement field to study a flexible hub–beam system with a tip mass. Cai[2] proposed a first-order approximation coupling model to study the dynamic characteristics of a hub-beam system with subjected to tip mass. Emam[3] studied the dynamics of a hub- geometrically nonlinear beam with a tip mass, and the hub was restrained by a translational and a rotational spring. Bai[4] applied the assumed mode method and Lagrangian principle to study the dynamics of a rotating hub-beam system with a tip mass. Ghaleh[5] researched the approximate solutions for dynamic characteristics of axially moving beam-like appendages with tip mass. Wei[6] proposed the global mode method to construct a reduced-order analytical dynamic model for a manipulator with tip mass. Ghaleh[7,8] investigated the deployment inertial effects of a space boom on its dynamic analysis and the dynamics of finite-mass satellites with a elastic boom.

Carrera's unified formulation (CUF) is a new general modeling theory proposed by Carrera for solving thin-walled beam models[9]. The main idea is to construct a three-dimensional displacement field of the beam by interpolating the displacement field of the section. The expression of the equation of motion is simplified by introducing the Einstein notation to construct the nucleus matrix. CUF is used to perform analysis of the statics problem[10] and the free vibration problem[11,12]. Results show that the CUF has a strong ability to study the shell-like properties of complex beam structures, especially thin-walled beam structures. Carrera[13] further extended the formula to analyze the effect of non-structural mass on thin-walled beams. Carrera[14] also used CUF to perform free vibration analysis of rotating structures.

In this paper, the dynamic characteristic of a rotating space tubular extendable boom is studied by using the one-dimensional Carrera's unified formulation, and the effect of the end mass, the base radius, and the angular velocity is valuated. Firstly, the coordinate systems and model assumptions of the boom are given based on the aerospace application background. Then, the dynamic models of the boom and the tip load are established by using CUF, and the equation of motion is expressed in the form of nucleus matrix. Finally, the dynamic characteristic of the boom is studied, and the effect of tip mass, base radius, and angular velocity is evaluated.

2 PROBLEM FORMULATION

The space tubular extendable boom is clamped to a satellite which is much heavier than the boom, and thus the satellite is modeled as a rotating rigid base of radius r_0. After deployment, the boom is formed into a slender, straight, and thin-walled configuration of length L_B. Figure 1 shows the cross-sectional circular configuration of the boom, and its arc is denoted by radius r_1, angle θ, and thinness h. The boom material is linearly elastic with Young's Modulus

E and Poisson's ratio ν. In all, the tubular extendable boom is modeled as a three-dimensional beam rotating around a fixed base.

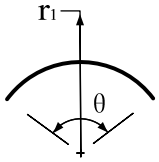

Figure 1: Cross-sectional circular configuration

2.1 Coordinate systems

Several Cartesian coordinate systems are established to describe the kinematics of the rotating beam, including inertial coordinate system, body-fixed coordinate system attached to the base and beam. The description of these coordinate system is as follows:

(1) Global coordinate system O-XYZ is an inertial coordinate system in uniform motion, serving as a reference system for the base motion.

(2) The body-fixed coordinate systems o-xyz and o_s-$x_s y_s z_s$ are attached to the satellite, and they are moving and rotating in the inertial space. The origins of coordinate systems o-xyz and are located at the base center and the boom root, respectively. Their motion with respect to the inertial coordinate system are described by the rotation angles of the base.

(3) The body-fixed coordinate system o_i-$x_i y_i z_i$ $(i=1,\cdots,n)$ is a local coordinate system attached to the ith beam element. When the finite element method is using for discretization, the relative position of each point on the beam element is described by the local coordinates whose origin is located at the element.

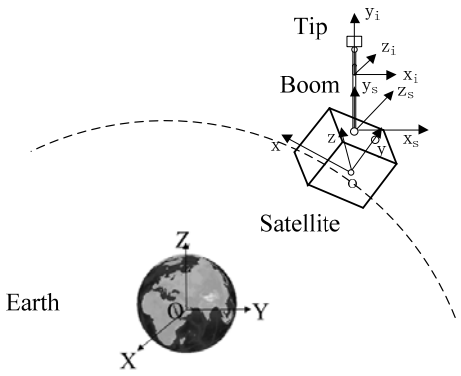

Figure 2: Description of the coordinate systems

2.2 Assumptions

To develop the kinematic description and dynamic equation of the tubular extendable boom, the following assumptions are postulated:

(1) The influence of the deployment mechanism is ignored. The mass and damping effect of the bolts are ignored. After deployment, the translational and rotational motion of the boom root are constrained.

(2) As for overall motion of the satellite, only rotation is considered to influence the boom

dynamics. Translation motion of the satellite is ignored, and the boom center line is assumed to be in the rotation plane of the satellite.

(3) The boom is assumed to maintain its stiffness after the deployment process. It is believed that the boom completely recovers its original structure and there is no residual stress. The influence of the space environment on boom stiffness is neglected.

(4) The boom deformation satisfies the small deformation assumption, and the material properties satisfy the generalized Hooke's law.

(5) Bending-torsional coupling and cross-sectional warping deformation is considered when modeling the thin-walled boom.

(6) The satellite is assumed to be moving in a uniform velocity on the orbit.

3 BOOM MODEL BY UNIFIED FORMULATION

3.1 Unified formulation

The unified formulation is adopted to describe the 3D displacement field of the beam. By using Einstein's notation to expand the generalized displacements above the cross-section, the displacement vector is expressed in a simple form as

$$\mathbf{u} = F_\tau \mathbf{u}_\tau, \quad \tau = 1,2,\ldots,M_u \tag{1}$$

where F_τ is expansion function depending on the cross-sectional coordinates; $\mathbf{u}_\tau$ stands for the generalized displacement vector depending on the axial coordinate; and M_u represents the number of expansion terms. For the circular cross-sectional beam studied in this paper, Taylor-like polynomials are chosen as the expansion functions[10]. The beam axis is assumed to be in the y direction, then F_τ is the function of x and z. Table 1 exhibits M_u and F_τ as functions of M.

Table 1: Expansion functions

N	N_u	F_τ
0	1	$F_1 = 1$
1	3	$F_2 = x \quad F_3 = y$
2	6	$F_4 = x^2 \quad F_5 = xy \quad F_6 = y^2$
3	10	$F_7 = x^3 \quad F_8 = x^2 y \quad F_9 = xy^2 \quad F_{10} = y^3$
…	…	…
N	$\frac{(M+1)(M+2)}{2}$	$F_{\frac{M^2+M+2}{2}} = x^M \quad F_{\frac{M^2+M+4}{2}} = x^{M-1}y \quad \ldots \quad F_{\frac{M(M+3)}{2}} = xy^{M-1} \quad F_{\frac{(M+1)(M+2)}{2}} = y^M$

When the finite element method is used to discretize the 3D beam, the displacement field could be expressed by shape functions N_i and the generalized nodal displacement vector $\mathbf{q}_{\tau i}$ as

$$\begin{aligned} &\mathbf{u}(x,y,z) = F_\tau(x,y) N_i(z) \mathbf{q}_{\tau i}, \qquad \mathbf{q}_{\tau i} = \left\{ q_{x\tau i}, q_{y\tau i}, q_{z\tau i} \right\}^{\mathrm{T}} \\ &\tau = 1,2,\ldots,M_u \qquad i = 1,2,\ldots,n \end{aligned} \tag{2}$$

3.2 Boom kinematics

As shown in figure 3, the hybrid coordinate method[15] is used to describe the overall motion of the 3D beam. For simplicity, the origin of the global coordinate system O-XYZ is moved to the base center. $\mathbf{r}_0$ and $\mathbf{r}$ are respectively the position vectors of the boom root and a beam point in the global coordinate system. $\boldsymbol{\rho}_0$ and $\boldsymbol{\rho}$ are the position vectors of a beam point before and after deformation in the body-fixed coordinate system o-xyz. $\mathbf{u}$ is the deformation vector in xyz frame.

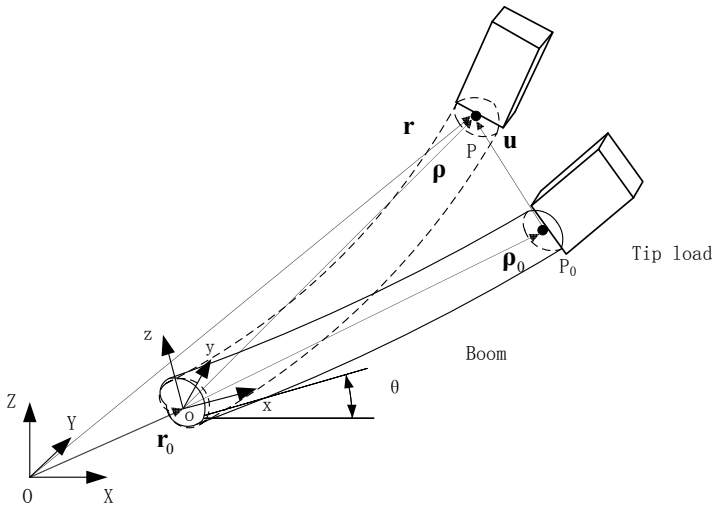

Figure 3: Kinematic model of the boom

Transformation between XYZ and xyz frames is related to the rotation angle θ. If the beam is rotating about the Z axis, then a transformation matrix is given by

$$\mathbf{A} = \begin{bmatrix} 1 & 0 & 0 \\ 0 & \cos\theta & -\sin\theta \\ 0 & \sin\theta & \cos\theta \end{bmatrix} \tag{3}$$

The position vector of the beam point in XYZ frame could be also expressed as

$$\mathbf{r} = \mathbf{r}_0 + \mathbf{A}\boldsymbol{\rho} = \mathbf{r}_0 + \mathbf{A}\left(\boldsymbol{\rho}_0 + \mathbf{u}\right) \tag{4}$$

The variation of the position vector $\mathbf{r}$, also known as the virtual displacement, is derived by

$$\delta\mathbf{r} = \delta\mathbf{r}_0 + \tilde{\mathbf{I}}\mathbf{A}\left(\boldsymbol{\rho}_0 + \mathbf{u}\right)\delta\theta + \mathbf{A}\delta\mathbf{u} \tag{5}$$

where $\tilde{\mathbf{I}}$ is an anti-symmetric matrix expressed by $\tilde{\mathbf{I}} = \begin{bmatrix} 0 & 0 & 0 \\ 0 & 0 & -1 \\ 0 & 1 & 0 \end{bmatrix}$

By introducing the unified formulation of displacement vector $\mathbf{u}$, the virtual displacement vector, the velocity vector and the acceleration vector are given by

$$\begin{aligned}
\delta\mathbf{r} &= \delta\mathbf{r}_0 + \tilde{\mathbf{I}}\mathbf{A}\left(\boldsymbol{\rho}_0 + F_\tau N_i \mathbf{q}_{\tau i}\right)\delta\theta + \mathbf{A}F_\tau N_i \delta\mathbf{q}_{\tau i} \\
\dot{\mathbf{r}} &= \dot{\mathbf{r}}_0 + \tilde{\mathbf{I}}\mathbf{A}\left(\boldsymbol{\rho}_0 + F_\tau N_i \mathbf{q}_{\tau i}\right)\dot{\theta} + \mathbf{A}F_\tau N_i \dot{\mathbf{q}}_{\tau i} \\
\ddot{\mathbf{r}} &= \ddot{\mathbf{r}}_0 + \tilde{\mathbf{I}}\mathbf{A}\left(\boldsymbol{\rho}_0 + F_\tau N_i \mathbf{q}_{\tau i}\right)\ddot{\theta} + \mathbf{A}F_\tau N_i \ddot{\mathbf{q}}_{\tau i} + \tilde{\mathbf{I}}^2\mathbf{A}\left(\boldsymbol{\rho}_0 + F_\tau N_i \mathbf{q}_{\tau i}\right)\dot{\theta}^2 + 2\tilde{\mathbf{I}}\mathbf{A}F_\tau N_i \dot{\mathbf{q}}_{\tau i}\dot{\theta}
\end{aligned} \tag{6}$$

3.3 Tip load kinematics

As shown in figure 4, the tip load and the boom are connected by two bolts. Almost no deformation occurs at the end of the boom and the end cross section could be modeled as a rigid body. The tip load is a cuboid with length l_F, width w_F, and height h_F.

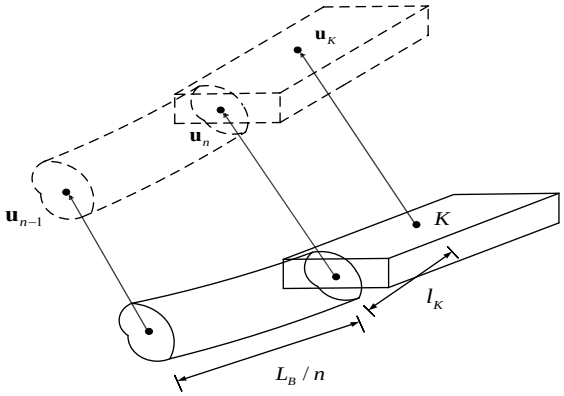

Figure 4: Kinematic model of the tip

By introducing the unified formulation of displacement vector $\mathbf{u}$, the displacement field on the end cross section could be written as

$$\mathbf{u}\left(x,L,z\right) = N_i F_\tau \mathbf{u}_{\tau i}\left(x,L,z\right) \tag{7}$$

The displacement vector of a tip load point K can be obtained by

$$\mathbf{u}_K = \mathbf{u}_n + nl_K\left(\mathbf{u}_n - \mathbf{u}_{n-1}\right)/L_B \tag{8}$$

where l_K is the distance from the point to the end cross section. The position vector of point K in XYZ frame is

$$\mathbf{r}_K = \mathbf{A}\boldsymbol{\rho}_K = \mathbf{A}\left(\mathbf{r}_0 + \boldsymbol{\rho}_0 + \mathbf{u}_K\right) \tag{9}$$

The virtual displacement vector, velocity vector, and acceleration vector are also derived by

$$\begin{aligned}
\delta\mathbf{r}_K &= \tilde{\mathbf{I}}\mathbf{A}\left(\mathbf{r}_0 + \boldsymbol{\rho}_0 + \mathbf{u}_K\right)\delta\theta + \mathbf{A}\delta\mathbf{u}_K \\
\dot{\mathbf{r}}_K &= \tilde{\mathbf{I}}\mathbf{A}\left(\mathbf{r}_0 + \boldsymbol{\rho}_0 + \mathbf{u}_K\right)\dot{\theta} + \mathbf{A}\dot{\mathbf{u}}_K \\
\ddot{\mathbf{r}}_K &= \tilde{\mathbf{I}}\mathbf{A}\left(\mathbf{r}_0 + \boldsymbol{\rho}_0 + \mathbf{u}_K\right)\ddot{\theta} + \mathbf{A}\ddot{\mathbf{u}}_K + \tilde{\mathbf{I}}^2\mathbf{A}\left(\mathbf{r}_0 + \boldsymbol{\rho}_0 + \mathbf{u}_K\right)\dot{\theta}^2 + 2\tilde{\mathbf{I}}\mathbf{A}\dot{\mathbf{u}}_K\dot{\theta}
\end{aligned} \tag{10}$$

4 EQUATIONS OF MOTION

Hamilton's principal is implemented to derive the dynamic equation of the beam in the form as

$$\int_{t_1}^{t_2}\left(-\delta T+\delta U-\delta W\right)dt=0 \tag{11}$$

where T, U, and W are the kinematic energy, potential energy, and the work done by external forces. δ represents variation.

The variation of the kinetic energy can be deduced by using the Lagrange equation:

$$\int_{t_1}^{t_2}-\delta T dt=\int_{t_1}^{t_2}\delta\left(\frac{1}{2}\int_{V_k}\rho\dot{\mathbf{r}}^{\mathrm{T}}\dot{\mathbf{r}}dV\right)dt=\int_{t_1}^{t_2}\left(\int_{V_k}\rho\delta\mathbf{r}^{\mathrm{T}}\ddot{\mathbf{r}}dV\right)dt \tag{12}$$

where $\mathbf{r}$, $\dot{\mathbf{r}}$, and $\ddot{\mathbf{r}}$ are the position vector, velocity vector, and acceleration vector of a point on the beam. The variation of the elastic potential energy could be divided into a linear part and a non-linear part. The linear part represents the variation of the elastic potential energy U_l, and the non-linear part is mainly composed by the variation of the centrifugal potential energy U_{nl}.

4.1 Variation of energies

The tip load is modeled as a rigid body, and its rotation motion is neglected. The tip mass has a great influence on the axial force of the beam. When calculating the nonlinear deformation energy of a beam, it is necessary to consider its contribution to the centrifugal force.

The variation of the tip load kinetic energy is given by

$$\begin{aligned}
&\int_{V_F}\rho_F\delta\mathbf{r}_K^{\mathrm{T}}\ddot{\mathbf{r}}_K dV=\Big[\delta\theta\int_{V_F}\rho_F\left(\boldsymbol{\rho}_0^{\mathrm{T}}+\mathbf{u}_k^{\mathrm{T}}\right)\tilde{\mathbf{I}}^T\tilde{\mathbf{I}}\left(\boldsymbol{\rho}_0+\mathbf{u}_k\right)dV\ddot{\theta}+\delta\theta\int_{V_F}\rho_F\left(\boldsymbol{\rho}_0^{\mathrm{T}}+\mathbf{u}_k^{\mathrm{T}}\right)\tilde{\mathbf{I}}^T dV\ddot{\mathbf{u}}_k\\
&+\delta\theta\int_{V_F}\rho_F\left(\boldsymbol{\rho}_0^{\mathrm{T}}+\mathbf{u}_k^{\mathrm{T}}\right)\tilde{\mathbf{I}}^T\tilde{\mathbf{I}}^2\left(\boldsymbol{\rho}_0+\mathbf{u}_k\right)dV\dot{\theta}^2+2\delta\theta\int_{V_F}\rho_F\left(\boldsymbol{\rho}_0^{\mathrm{T}}+\mathbf{u}_k^{\mathrm{T}}\right)\tilde{\mathbf{I}}^T\tilde{\mathbf{I}}\dot{\mathbf{u}}_k dV\dot{\theta}\\
&+\delta\mathbf{u}_k^{\mathrm{T}}\int_{V_F}\rho_F\tilde{\mathbf{I}}\left(\boldsymbol{\rho}_0+\mathbf{u}_k\right)dV\ddot{\theta}+\delta\mathbf{u}_k^{\mathrm{T}}\int_{V_F}\rho_F dV\ddot{\mathbf{u}}_k+\delta\mathbf{u}_k^{\mathrm{T}}\int_{V_F}\rho_F\tilde{\mathbf{I}}^2\left(\boldsymbol{\rho}_0+\mathbf{u}_k\right)dV\dot{\theta}^2+2\delta\mathbf{u}_k^{\mathrm{T}}\int_{V_F}\rho_F\tilde{\mathbf{I}}\dot{\mathbf{u}}_k dV\dot{\theta}
\end{aligned} \tag{13}$$

The variation of the beam kinetic energy is given by

$$\begin{aligned}
&\sum_{k=1}^{N_B}\int_{V_k}\rho\delta\mathbf{r}^{\mathrm{T}}\ddot{\mathbf{r}}dV=\sum_{k=1}^{N_B}\Big[\delta\theta\int_{V_k}\rho\left(\boldsymbol{\rho}_0^T+F_\tau N_i\mathbf{q}_{\tau i}^T\right)\tilde{\mathbf{I}}^T\tilde{\mathbf{I}}\left(\boldsymbol{\rho}_0+F_s N_j\mathbf{q}_{sj}\right)dV\ddot{\theta}\\
&+\delta\theta\int_{V_k}\rho\left(\boldsymbol{\rho}_0^T+F_\tau N_i\mathbf{q}_{\tau i}^T\right)\tilde{\mathbf{I}}^T F_s N_j\ddot{\mathbf{q}}_{sj}dV+\delta\theta\int_{V_k}\rho\left(\boldsymbol{\rho}_0^T+F_\tau N_i\mathbf{q}_{\tau i}^T\right)\tilde{\mathbf{I}}^T\tilde{\mathbf{I}}^2\left(\boldsymbol{\rho}_0+F_s N_j\mathbf{q}_{sj}\right)dV\dot{\theta}^2\\
&+2\delta\theta\int_{V_k}\rho\left(\boldsymbol{\rho}_0^T+F_\tau N_i\mathbf{q}_{\tau i}^T\right)\tilde{\mathbf{I}}^T\tilde{\mathbf{I}}F_s N_j\dot{\mathbf{q}}_{sj}dV\dot{\theta}+\int_{V_k}\delta\mathbf{q}_{\tau i}^T\rho F_\tau N_i\tilde{\mathbf{I}}\left(\boldsymbol{\rho}_0+F_s N_j\mathbf{q}_{sj}\right)dV\ddot{\theta}+\delta\mathbf{q}_{\tau i}^T\int_{V_k}\rho F_\tau N_i F_s N_j dV\ddot{\mathbf{q}}_{sj}\\
&+\delta\mathbf{q}_{\tau i}^T\int_{V_k}\rho F_\tau N_i\tilde{\mathbf{I}}^2\left(\boldsymbol{\rho}_0+F_s N_j\mathbf{q}_{sj}\right)dV\dot{\theta}^2+\delta\mathbf{q}_{\tau i}^T 2\int_{V_k}\rho F_\tau N_i\tilde{\mathbf{I}}F_s N_j\dot{\mathbf{q}}_{sj}dV\dot{\theta}\Big]
\end{aligned} \tag{14}$$

The variation of the beam linear potential energy is directly given in literature[10].

The centrifugal stress in the boom can be obtained by D'Alembert's principle:

$$\sigma=T\left(y\right)/S=T_n/S+\rho\Omega^2\left(r_0L_B+\frac{1}{2}L_B^2-r_0y-\frac{1}{2}y^2\right) \tag{15}$$

The variation of the nonlinear strain energy is obtained by

$$\delta U_{nl}=\delta\mathbf{q}_{\tau i}\sum_{k=1}^{N_B}\left[\int_{V_k}F_\tau N_{i,y}F_s N_{j,y}M_l\Omega^2dV\right]\mathbf{q}_{sj} \tag{16}$$

where $M_l = \rho\left(r_0 L_B + \frac{1}{2}L_B^2 - r_0 y - \frac{1}{2}y^2\right) + m_F\left(r_0 + L_B + l_F/2\right)/S$.

In the above formulation, Ω is the rotation velocity, and S is cross-sectional area.

4.2 Dynamic equation

The dynamic equation of the beam is obtained by using the Hamilton's principal. To further simplify the form of the equation, the integral and matrix notations are introduced by

$$\mathbf{I}_{ny} = \begin{bmatrix} 0 & 1 & 0 \\ 1 & 0 & 0 \\ 0 & 0 & 1 \end{bmatrix}, \qquad \lhd \cdots \rhd = \int_S \cdots dS, \qquad \mathbf{\Omega} = \begin{bmatrix} 0 & 0 & 0 \\ 0 & 0 & -\Omega \\ 0 & \Omega & 0 \end{bmatrix}$$
$$\left(I_L^i, I_L^{ij}, I_L^{i_y j}, I_L^{ij_y}, I_L^{i_y j_y}\right) = \int_L \left(N_i, N_i N_j, \frac{dN_i}{dy} N_j, N_i \frac{dN_j}{dy}, \frac{dN_i}{dy}\frac{dN_j}{dy}\right) dy \tag{17}$$

When no external force is applied, the dynamic equation of a beam element is obtained as

$$\mathbf{M}^{ij\tau s}\ddot{\mathbf{q}}_{sj} + \mathbf{G}^{ij\tau s}\dot{\mathbf{q}}_{sj} + \mathbf{K}_{TOT}^{ij\tau s}\mathbf{q}_{sj} + \mathbf{F}_{TOT}^{i\tau} = \mathbf{0} \tag{18}$$

where $\mathbf{M}^{ij\tau s}$, $\mathbf{G}^{ij\tau s}$, $\mathbf{K}_{\mathrm{TOT}}^{ij\tau s}$, $\mathbf{F}_{\mathrm{TOT}}^{i\tau}$ are the mass matrix, Coriolis matrix, the total stiffness matrix, the total force matrix in the form of the fundamental nucleus, repectively.

$\mathbf{M}^{ij\tau s}$ is an symmetric matrix expressed as

$$\begin{aligned}
&\mathbf{M}^{ij\tau s} = \rho I_k^{ij} \lhd F_\tau \mathbf{I} F_s \rhd \qquad (1 \le i, j \le n-2) \\
&\mathbf{M}^{(n-1)(n-1)\tau s} = \left(\rho + \rho_F n^2 l_F^2 / L_B^2\right) I_k^{ij} \lhd F_\tau \mathbf{I} F_s \rhd \\
&\mathbf{M}^{(n-1)n\tau s} = \mathbf{M}^{n(n-1)\tau s} = \left(\rho - \rho_F n l_F \left(L_B + n l_F\right)/L_B^2\right) I_k^{ij} \lhd F_\tau \mathbf{I} F_s \rhd \\
&\mathbf{M}^{nn\tau s} = \left(\rho + \rho_F \left(L_B + n l_F\right)^2 / L_B^2\right) I_k^{ij} \lhd F_\tau \mathbf{I} F_s \rhd
\end{aligned} \tag{19}$$

$\mathbf{G}^{ij\tau s}$ is an antisymmetric matrix expressed as

$$\begin{aligned}
&\mathbf{G}^{ij\tau s} = \rho I_k^{ij} \lhd F_\tau \mathbf{I} F_s \rhd 2\mathbf{\Omega}, \qquad (1 \le i, j \le n-2) \\
&\mathbf{G}^{(n-1)(n-1)\tau s} = \left(\rho - \rho_F n l_F / L_B\right) I_k^{ij} \lhd F_\tau \mathbf{I} F_s \rhd 2\mathbf{\Omega} \\
&\mathbf{G}^{nn\tau s} = \left(\rho + \rho_F \left(L_B + n l_F\right)/L_B\right) I_k^{ij} \lhd F_\tau \mathbf{I} F_s \rhd 2\mathbf{\Omega}
\end{aligned} \tag{20}$$

$\mathbf{K}_{\mathrm{TOT}}^{ij\tau s} = \mathbf{K}_l^{ij\tau s} + \mathbf{K}_{nl}^{ij\tau s} + \mathbf{K}_{\Omega}^{ij\tau s} + \mathbf{K}_{\dot{\Omega}}^{ij\tau s}$, where $\mathbf{K}_l^{ij\tau s}$ and $\mathbf{K}_{nl}^{ij\tau s}$ are the linear and nonlinear stiffness matrix, and $\mathbf{K}_{\Omega}^{ij\tau s}$ and $\mathbf{K}_{\Omega}^{ij\tau s}$ are the centrifugal softening matrix and the inertial stiffness matrix resulting from rotational angular velocity and rotational angular acceleration. These matrixes are expressed as

$$\begin{aligned}
\mathbf{K}_l^{ij\tau s} =& \lhd F_\tau \mathbf{D}_p^T \tilde{\mathbf{C}}_{pp} \mathbf{D}_p F_s \rhd I_L^{ij} + \lhd F_\tau \mathbf{D}_p^T \tilde{\mathbf{C}}_{pn} \mathbf{D}_{n\Omega} F_s \rhd I_L^{ij} + \lhd F_\tau \mathbf{D}_p^T F \rhd \tilde{\mathbf{C}}_{pn} I_L^{ij_y} \mathbf{I}_{ny} \\
&+ \lhd F_\tau \mathbf{D}_{n\Omega}^T \tilde{\mathbf{C}}_{np} \mathbf{D}_p F_s \rhd I_L^{ij} + \lhd F_\tau \mathbf{D}_p F_s \rhd \tilde{\mathbf{C}}_{np} I_L^{i_y j} \mathbf{I}_{ny}^T + \lhd F_\tau \mathbf{D}_{n\Omega}^T \tilde{\mathbf{C}}_{nn} \mathbf{D}_{n\Omega} F_s \rhd I_L^{ij} \\
&+ \lhd F_\tau \mathbf{D}_{n\Omega} F_s \rhd \tilde{\mathbf{C}}_{nn} I_L^{i_y j} \mathbf{I}_{ny}^T + \lhd F_\tau \mathbf{D}_{n\Omega}^T F_s \rhd I_L^{ij_y} \mathbf{I}_{ny} + \lhd F_\tau F_s \rhd \tilde{\mathbf{C}}_{nn} I_L^{i_y j_y} \mathbf{I}_{ny}^T \mathbf{I}_{ny}{}_n^{ij\tau s}
\end{aligned} \tag{21}$$

$$\begin{aligned}
\mathbf{K}_{nl}^{ij\tau s} &= \rho\Omega^2 I_k^{i,y\,j,y\sigma} \lhd F_\tau F_s \rhd \\
\mathbf{K}_{\Omega}^{ij\tau s} &= -\rho I_l^{ij} \lhd F_\tau \mathbf{I} F_s \rhd \boldsymbol{\Omega}^{\mathrm{T}}\boldsymbol{\Omega} - \int_{V_F} \rho_F \left(\boldsymbol{\rho}_0 + \mathbf{u}_k\right) dV \boldsymbol{\Omega}^{\mathrm{T}}\boldsymbol{\Omega} \\
\mathbf{K}_{\dot{\Omega}}^{ij\tau s} &= \rho I_k^{ij} \lhd F_\tau \mathbf{I} F_s \rhd \dot{\boldsymbol{\Omega}} + 2\int_{V_F} \rho_F \dot{\mathbf{u}}_k dV \dot{\boldsymbol{\Omega}}
\end{aligned} \tag{22}$$

$\mathbf{F}_{\mathrm{TOT}}^{i\tau} = \mathbf{F}_{\Omega\mathbf{r}}^{i\tau} + \mathbf{F}_{\dot{\Omega}\mathbf{r}}^{i\tau}$, where $\mathbf{F}_{\Omega\mathbf{r}}^{i\tau}$ and $\mathbf{F}_{\dot{\Omega}\mathbf{r}}^{i\tau}$ are the centrifugal force matrix and the inertia force matrix resulting from the rotational angular velocity and the rotational angular acceleration, respectively. These matrixes are expressed as

$$\begin{aligned}
\mathbf{F}_{\Omega\mathbf{r}}^{i\tau} &= -\rho I_l^i \boldsymbol{\Omega}^{\mathrm{T}}\boldsymbol{\Omega} \lhd F_\tau \mathbf{I}\mathbf{r} \rhd, \qquad (1 \le i, j \le n-2) \\
\mathbf{F}_{\Omega\mathbf{r}}^{(n-1)\tau} &= -I_l^i \boldsymbol{\Omega}^{\mathrm{T}}\boldsymbol{\Omega} \lhd F_\tau \mathbf{I}\left(\rho - \rho_F n l_F / L_B\right)\mathbf{r} \rhd \\
\mathbf{F}_{\Omega\mathbf{r}}^{n\tau} &= -I_l^i \boldsymbol{\Omega}^{\mathrm{T}}\boldsymbol{\Omega} \lhd F_\tau \mathbf{I}\left(\rho + \rho_F \left(L_B + n l_F\right)/L_B\right)\mathbf{r} \rhd \\
\mathbf{F}_{\dot{\Omega}\mathbf{r}}^{i\tau} &= \rho I_l^i \dot{\boldsymbol{\Omega}} \lhd F_\tau \mathbf{I}\mathbf{r} \rhd, \qquad (1 \le i, j \le n)
\end{aligned} \tag{23}$$

5 RESULTS AND DISCUSSION

The natural frequencies of the boom with tip load are analyzed in this paper. A typical space tubular extendable boom is studied. The boom length L_B is 1200mm, and the cross-sectional arc has a radius r_1 of 13.3mm, an angle θ of 1.85rad, and a thinness h of 0.1mm. The ratio of base radius to boom length $\delta=r_0/L_B$ is selected as 0, 1, 2 and 3, and the ratio of tip mass to boom mass $\omega = m_t / m_B$ is selected as 0, 1, and 5. In order to theoretically study the dynamic characteristics of the boom with tip load at various angular velocity, a large range of angular velocities are selected for the study. In this paper, the selection is 0-20 rad/s.

Figure 5-7 shows the relationship between the first 5 natural frequencies and the angular velocity at different base radius and tip mass. The natural frequencies generally increase with the angular velocity, but they may diminish at certain angular velocity, especially the low-order ones. For example, given ω=1 and δ=0, in the vicinity of the angular velocity of 10.2 rad/s, the first order natural frequency rapidly decreases to close to zero. According to literature on rotor dynamics[16,17], this angular velocity represents the first order critical velocity of the rotating structure, where the structure may experience resonance and large deformation. When accelerating the angular velocity, the structural natural frequencies quickly recover to their normal values. Higher orders of critical velocity may exist when ω becomes larger. When ω=1 and δ=0, the rotating structure has a first order critical velocity of 3.2 rad/s, and a second order critical velocity of 7.8 rad/s.

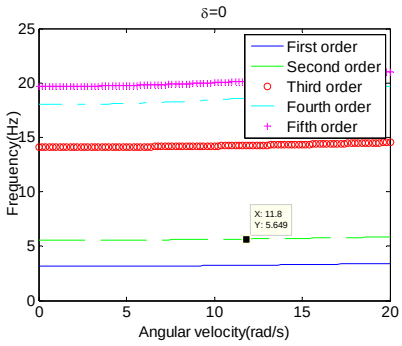

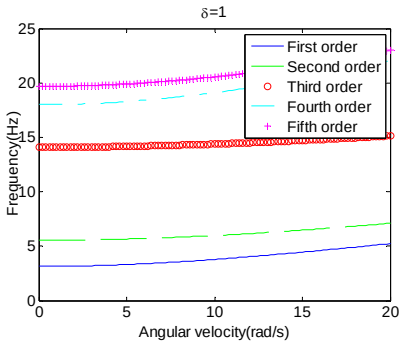

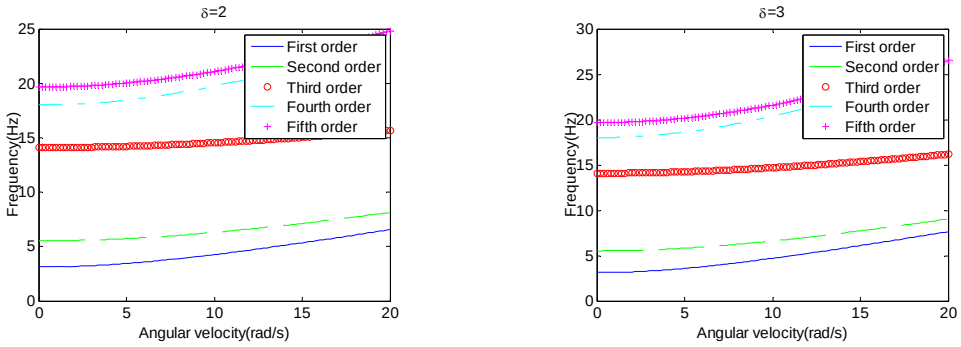

Figure 5: Natural frequencies of the boom with tip load when $\omega = 0$

When figure 6 and 7 are compared to figure 5, it is found that the mass effect of the tip load reduces the natural frequencies of the boom, especially the low-order ones. For the static natural frequencies, when ω is selected as 1, the first 5 order are reduced from 3.134Hz, 5.535Hz, 14.09Hz, 18.01Hz, 19.67Hz by 55.07%, 47.52%, 54.13%, 28.82%, and 24.50%, respectively. In addition, heavier tip mass leads to more reduction of natural frequencies. When ω=5, the first three natural frequencies have been reduced by even more than 78%. Heavier tip load also results in lower critical velocity. When ω rises from 1 to 5, The first order critical velocity =1 is reduced from 10.2rad/s to 4.4rad/s when δ=0, and from 13.2rad/s to 4.6rad/s when δ=1.

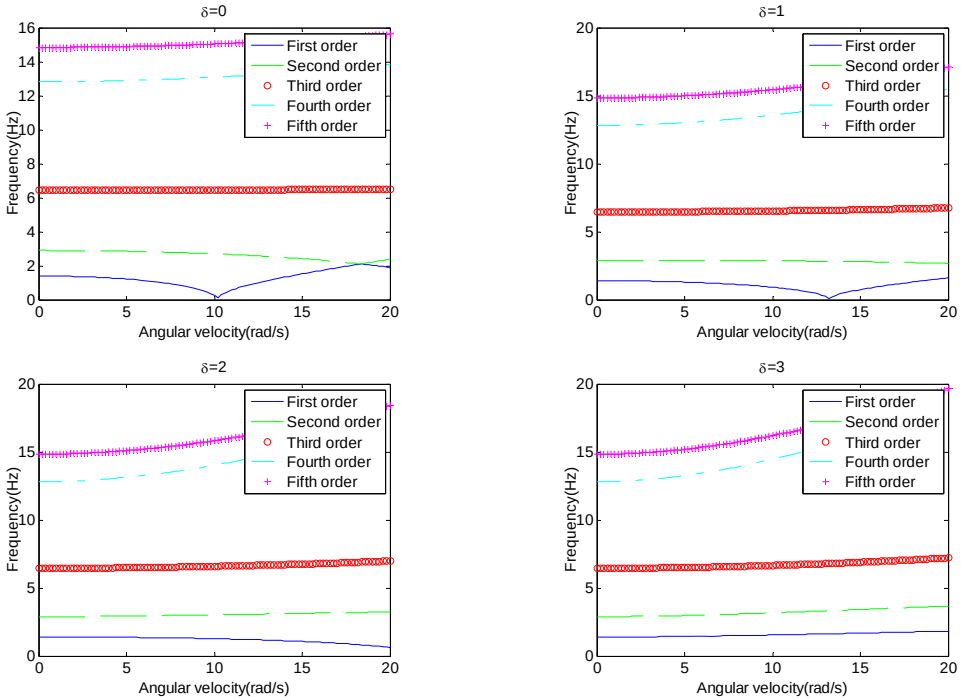

Figure 6: Natural frequencies of the boom with tip load when $\omega = 1$

It is obvious to conclude from the figure 5-7 that the natural frequencies and the critical velocities have been improved by larger base radius. With respect to the natural frequencies,

when ω=0 and Ω=20rad/s, an increase of δ from 0 to 1, 2, 3 gives improvements of the first order natural frequencies by 53.15%, 91.89%, and 123.88%, respectively. For critical velocities, when ω=1, an increase of δ from 0 to 1 has improved the first order critical velocity from 10.2rad/s to 13.2 rad/s. When δ is selected as 2 or 3, the first order critical velocity rises beyond 20rad/s. When ω=10, an increase of δ from 0 to 1, 2, 3 improves the first order critical velocity from 4.4 to 4.6, 4.8, and 5.0, and the second order critical velocity from 11.0 to 11.8, 12.6, and 13.4, respectively. To conclude, larger base radius can improve the dynamic characteristics of the rotating boom.

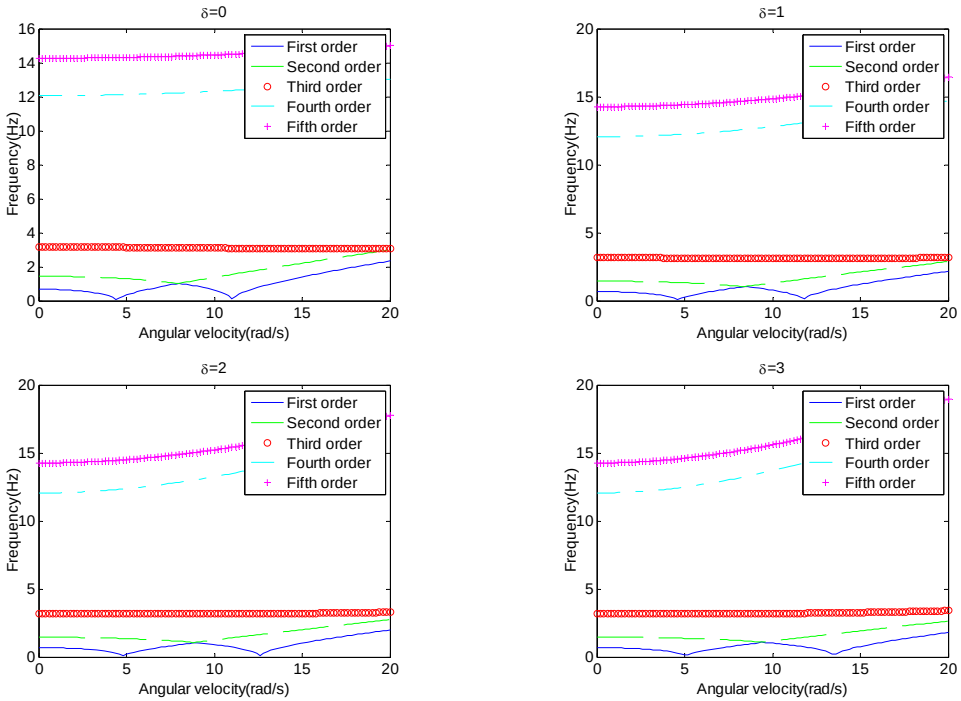

Figure 7: Natural frequencies of the boom with tip load when $\omega = 5$

6 CONCLUSION

- The low order natural frequencies diminish rapidly at the critical velocity, where the first order natural frequency is close to zero and the structure suffers from resonance and large deformation. To ensure the structural safety, the angular velocity of the satellite needs to be controlled less than the first order critical velocity of the boom.
- The mass effect of the tip load reduces the natural frequencies of the boom, especially the low-order ones. Heavier tip mass results in lower critical velocities and natural frequencies. So the boom needs to be carefully designed to match the designed tip load, angular velocity and base radius of the satellite.
- To some extent, larger base radius can improve the dynamic characteristics of the rotating structure. Thus, placing the boom root far from the satellite center is helpful to the structural safety.

7 ACKNOWLEDGMENTS

This work is supported by the Major Program of National Natural Science Foundation of China under Grant Numbers 51675525, 61690210 and 61690213.

REFERENCES

[1] Yang, H.; Hong, J.; Yu, Z. Dynamics modelling of a flexible hub – beam system with a tip mass. *Journal of Sound & Vibration* (2003), 266: 759-774.

[2] Cai, G. P.; Hong, J. Z.; Yang, S. X. Dynamic analysis of a flexible hub-beam system with tip mass. *Mechanics Research Communications* (2005), 32: 173-190.

[3] Emam, S. A. Dynamics of a Flexible-hub Geometrically Nonlinear Beam with a Tip Mass. *Journal of Vibration & Control* (2010), 16: 1989-2000.

[4] Bai, S.; Ben-Tzvi, P.; Zhou, Q.; Huang, X. Dynamic modeling of a rotating beam having a tip mass. *International Workshop on Robotic and Sensors Environments*. (2008): 52-57.

[5] Ghaleh, P. B.; Khayyat, A. A.; Farjami, Y.; Abedian, A. Approximate analytical solutions of an axially moving spacecraft appendage subjected to tip mass. *Proceedings of the Institution of Mechanical Engineers Part G Journal of Aerospace Engineering* (2014), 228: 1487-1497.

[6] Wei, J.; Cao, D.; Liu, L.; Huang, W. Global mode method for dynamic modeling of a flexible-link flexible-joint manipulator with tip mass. *Applied Mathematical Modelling* (2017), 48.

[7] Ghaleh, P. B.; Malaek, S. M. On dynamic stiffness of spacecraft flexible appendages in deployment phase. *Aerospace Science & Technology* (2015), 47: 1-9.

[8] Ghaleh, P. B.; Malaek, S. M.; Abedian, A. On the coupled dynamics of small spacecraft and elastic deployable appendages. *Multibody System Dynamics* (2016), 40: 1-26.

[9] Erasmo Carrera, A. P. M. P. Recent developments on refined theories for beams with applications. *Mechanical Engineering Reviews* (2015).

[10] Carrera, E.; Giunta, G.; Nali, P.; Petrolo, M. Refined beam elements with arbitrary cross-section geometries. *Computers & Structures* (2010), 88: 283-293.

[11] Carrera, E.; Petrolo, M.; Nali, P. Unified formulation applied to free vibrations finite element analysis of beams with arbitrary section. *Shock and Vibration* (2011): 485-502.

[12] Pagani, A.; Boscolo, M.; Banerjee, J. R.; Carrera, E. Exact dynamic stiffness elements based on one-dimensional higher-order theories for free vibration analysis of solid and thin-walled structures. *Journal of Sound and Vibration* (2013), 332: 6104-6127.

[13] Carrera, E.; Pagani, A.; Zangallo, F. Thin-walled beams subjected to load factors and non-structural masses. *International Journal of Mechanical Sciences* (2014), 81: 109-119.

[14] Carrera, E.; Filippi, M.; Zappino, E. Free vibration analysis of rotating composite blades via Carrera Unified Formulation. *Composite Structures* (2013), 106: 317-325.

[15] Zienkiewicz, O. C.; Taylor, R. L. The Finite Element Method, Fourth Edition, Volume 1, Basic Formulation and Linear Problems. *International Journal for Numerical Methods in Engineering* (1994), 12: 1597-1615.

[16] Dimarogonas, A. D.; Paipetis, S. A.; Chondros, T. G. *Analytical Methods in Rotor Dynamics*. Applied Science Publishers, (1983).

[17] Childs, D. W. Turbomachinery Rotordynamics: Phenomena, Modeling, and Analysis. *Turbomachinery Rotordynamics Phenomena Modeling & Analysis* (1995), 28: 262-263.